



Official English translation

Complex dynamics and chaos in electronic self-oscillator with saturation mechanism provided by parametric decay

S. P. Kuznetsov^{1,2}, L. V. Turukina^{1,2}

¹Kotelnikov Institute of Radio-Engineering and Electronics of RAS, Saratov Branch
38, Zelenaya, 410019 Saratov, Russia

²Saratov State University
83, Astrakhanskaya, 410012 Saratov, Russia
E-mail: spkuz@yandex.ru, lvtur@rambler.ru

Received 22.09.2017

We consider an electronic oscillator based on two LC-circuits, one of which includes negative conductivity (the active LC-circuit), where complex dynamics and chaos occur corresponding to the model of wave turbulence of Vyshkind–Rabinovich. The saturation effect for the self-oscillations and their chaotisation take place due to parametric mechanisms due to the presence of a quadratic nonlinear reactive element based on an operational amplifier and an analog multiplier.

The study is based on combination of circuit simulation with the use of the software product Multisim and of numerical computations with equations that directly describe the oscillations of voltages and currents in the oscillatory circuit, amplitude equations, and the equations represented in the form suggested by S.Y. Vyshkind and M.I. Rabinovich.

For all these models, time dependences of dynamic variables are presented as well as portraits of attractors, and Lyapunov exponents depending on parameters. For the Vyshkind–Rabinovich model we additionally present a chart of dynamic regimes in the parameter plane. It is shown that all models demonstrate transitions to chaos through period-doubling bifurcation scenario observed under decrease in the supercriticality parameter in the active LC-circuit. The resulting chaotic attractor is similar in structure to the Rössler attractor.

The proposed scheme allows observing in the electronic device chaotic dynamics of the resonant triplet under instability of the high-frequency mode, considered in due time by Vyshkind and Rabinovich and interpreted as a model of a certain type of wave turbulence in dissipative media. The presented results testify a possibility of using the considered electronic circuit for analog simulation of oscillatory and wave phenomena in systems to which the Vyshkind–Rabinovich model is applicable.

Key words: parametric mode interaction, chaotic attractor, auto-oscillations, analog simulation.

<https://doi.org/10.18500/0869-6632-2018-26-1-33-47>

References: Complex dynamics and chaos in electronic self-oscillator with saturation mechanism provided by parametric decay. *Izvestiya VUZ, Applied Nonlinear Dynamics*, 2018, vol. 26, iss. 1, pp. 33–47. <https://doi.org/10.18500/0869-6632-2018-26-1-33-47>

Introduction

Three-wave parametric interaction of oscillations and waves in systems with quadratic nonlinearity takes place in plasma physics, nonlinear optics, acoustics, electronic engineering. A general model covering situations of different physical nature is the system referred to as a resonance triplet, meaning the weak interaction in quadratic nonlinearity of three oscillation modes, the frequencies of which are subject to condition of parametric resonance $\omega_2 = \omega_1 + \omega_0$.

If the system has a high-frequency mode excitation due to linear instability and low-frequency modes are characterized by attenuation, then at a certain level of amplitudes in the dynamics of the resonant triplet there is a saturation of oscillations, defined, as it is said to be, by parametric decay. Vyshkind and Rabinovich [1] have shown that in this situation the dynamics can become chaotic, moreover, transition to chaos due to a parameter change is carried out through a cascade of period-doubling bifurcations of self-oscillating regimes.

In the simplest case, that of degenerate parametric resonance, frequencies ω_0 and ω_1 are the same, so that the frequency condition takes the form $\omega_2 = 2\omega_1$, and the problem is reduced to considering the interaction between the two modes. This assumption facilitates scrutiny and makes the analysis more observable, as the dynamics depends on fewer parameters. For this case, Vyshkind and Rabinovich have derived and analyzed a model by a system of three first-order differential equations, considering it justifiable to be interpreted as a model of a certain type of wave turbulence in dissipative media. This model is now recognized as a classical example of small-dimensional systems that demonstrate dynamic chaos.

The problem of resonance triplet dynamics under high-frequency mode instability might be considered as a generalization covering systems of different physical nature, many of which have an obvious applied significance. In particular, several works in nonlinear optics devoted to spin waves in magnetic films and processes related to the second harmonic generation [2–6] are worth to be mentioned.

For example, in paper [2] modulation instability of spin waves in magnetic membrane under three-magnon decay is studied, mechanisms of this phenomenon and stochasticization of the envelope under self-modulation are determined. Paper [3] presents an experimental study of ring self-oscillating system based on a ferromagnetic structure in the case where three-magnon decay processes are allowed; on the basis of the constructed model are calculated characteristic modes of generation, including chaotic sequence of microwave pulses. The results of numerical simulation are compared with experimental data. In paper [4], a simple model of nonlinear saturation in unstable mode is studied and it is shown that as the attenuation in the system increases, the transition to chaos through a sequence of bifurcations takes place. This is explained on the basis of one-dimensional map, which is numerically derived from the original system of differential equations.

We consider the possibility of analog modeling for dynamic phenomena natural and useful. This could be done by applying the simplest representative of the systems enclosed in this generalization because it is convenient both for implementation and experimental research. Therefore, the simple electronic circuit proposed in this paper is of primary concern. It is a scheme based on two oscillatory circuits, one of which includes negative conductivity, and there is a specially designed reactive nonlinear element with a characte-

ristic almost exactly given by the quadratic function, which was previously used in another system with parametric interaction of modes [7]. Theoretical description of the scheme leads to equations coinciding with the Vyskind–Rabinovich turbulence model [1].

1. Scheme of the parametric generator

Let us consider fig. 1, showing a circuit consisting of two oscillating circuits, one of which includes negative conductivity provided by connection of the operational amplifier OA2.

The saturation effect of self-oscillations and their chaotization is caused by the parametric mechanism due to the presence of a quadratic nonlinear reactive element based on the operational amplifier OA1 and analog multiplier A1. When voltage U is applied to the input of this element, a potential relative to ground occurs at both input terminals of the operational amplifier. Since in theory the input impedance of the operational amplifier is infinite, the presence of current U/R through resistor R_5 , having a grounded conductor, implies the same current passing through resistor R_4 , connected with it, therefore, voltage at the input of the analog multiplier A1 should be equal to $2U$. Accordingly, at the output there should be voltage $4KU^2$, where K is the transmission coefficient with dimension of reverse voltage. Currents flowing through two capacitors C_0 , amount $C_0 dU/dt$ and $(d/dt)(4KU^2 - C_0U)$, giving a total current through the nonlinear element \tilde{C} .

Without regard to dissipation, we assume the eigenfrequencies of the oscillatory circuits to satisfy, at least approximately, the conditions of the parametric resonance

$$\Omega_2 \approx \Omega_1. \tag{1}$$

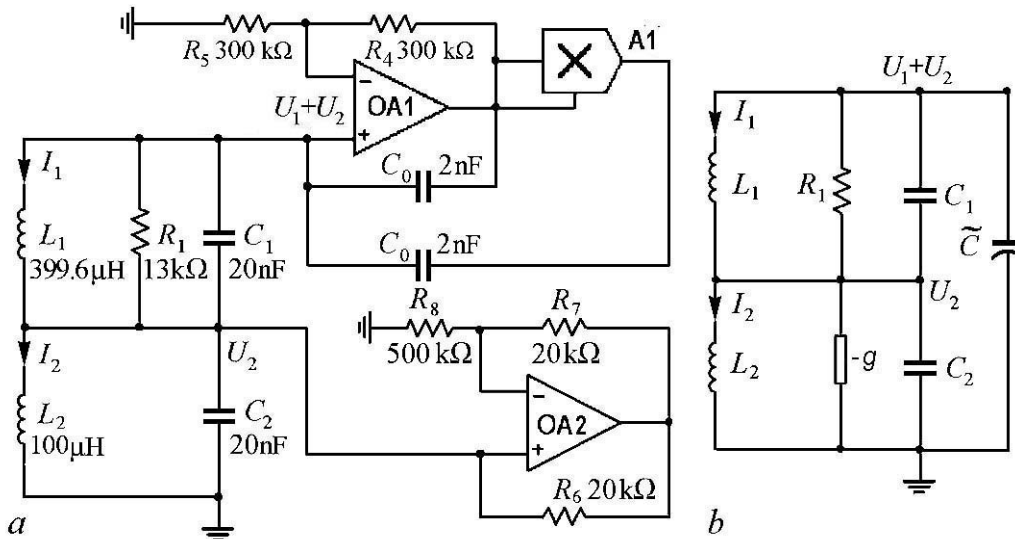


Fig. 1. The scheme of the parametric chaos generator (a) and its equivalent scheme (b), $(-g)=1/R_g$ is negative conductivity, the presence of which is provided by the presence of an operational amplifier OA2, \tilde{C} is reactive element (it is a two-terminal network with a quadratic nonlinearity realized using an operational amplifier OA1). Multiplier transfer factor A1 is $K = 1/8 \text{ V}^{-1}$

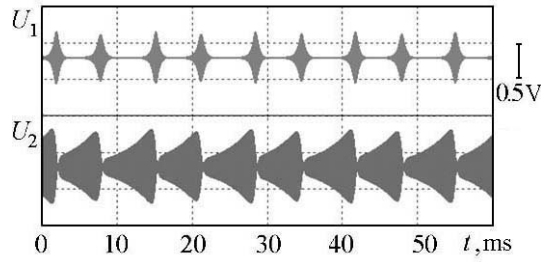


Fig. 2. A typical type of time dependences of voltage on capacitors C_1 and C_2 obtained by simulation of the scheme in the Multisim with $R_8 = 500 \text{ k}\Omega$. The other nominal values of the components are shown in Fig. 1

Fig. 2 shows graphs of voltage realization for capacitors C_1 и C_2 , obtained using the virtual oscilloscope for circuit simulation in Multisim environment with component values specified in the figure caption. A mode of nonlinear oscillations follows the transition process. In the given scale the high-frequency completion is indistinguishable, but the irregular, apparently, chaotic amplitude dynamics is observable.

Within circuit simulation in Multisim environment it is difficult to identify some significant features of dynamics, including the expected presence of a chaotic attractor, and to determine such characteristics as the Lyapunov exponents; therefore, in the following sections we consider the equations describing the system and analyze the results of their numerical solution.

2. Basic equations for the parametric generator

Let U_1, U_2 be voltages on capacitors C_1 и C_2 , having the same capacity C , let I_1, I_2 be currents going through inductors L_1 and L_2 . Kirchhoff's equations are written as

$$\begin{aligned} L_1 \dot{I}_1 &= U_1, \\ L_2 \dot{I}_2 &= U_2, \\ C \dot{U}_1 + U_1/R_1 + I_1 &= -I, \\ C \dot{U}_2 + U_2/R_2 + I_2 &= -I, \end{aligned} \quad (2)$$

where I is the current going through a nonlinear element defined by the expression

$$I = \frac{d}{dt} 4KC_0 U^2 = \varepsilon \frac{dU^2}{dt}. \quad (3)$$

Here $\varepsilon = 8KC_0/C$, $C = C_1 = C_2$, and

$$U = U_1 + U_2. \quad (4)$$

These equations can also be rewritten as

$$\begin{aligned} \frac{d^2}{dt^2} \left(U_1 + \frac{1}{2} \varepsilon U^2 \right) + \frac{1}{R_1 C} \frac{dU_1}{dt} + \frac{U_1}{L_1 C} &= 0, \\ \frac{d^2}{dt^2} \left(U_2 + \frac{1}{2} \varepsilon U^2 \right) - \frac{g}{C} \frac{dU_2}{dt} + \frac{U_2}{L_2 C} &= 0. \end{aligned} \quad (5)$$

Let us introduce a normalized non-dimensional time $t' = t/(2R_1C)$. Then the equations can be rewritten as

$$\begin{aligned}\ddot{X}_1 + 2\dot{U}_1 + \Omega_1^2 U_1 &= 0, \\ \ddot{X}_2 - 2\gamma\dot{U}_2 + \Omega_2^2 U_2 &= 0, \\ X_{1,2} &= U_{1,2} + \frac{1}{2}\varepsilon U^2,\end{aligned}\tag{6}$$

$$\gamma = gR_1 = \frac{R_1}{R_g}, \quad \Omega_{1,2} = 2R_1\sqrt{\frac{C}{L_{1,2}}},\tag{7}$$

where dots represent derivatives in non-dimensional time. For the numerical solution it is convenient to rewrite them in the form of a first order system:

$$\begin{aligned}\dot{Y}_1 &= -\Omega_1 U_1, & \dot{X}_1 &= \Omega_1 Y_1 - 2U_1, \\ \dot{Y}_2 &= -\Omega_2 U_2, & \dot{X}_2 &= \Omega_2 Y_2 + 2\gamma U_2, \\ U_{1,2} &= X_{1,2} - \frac{1}{2}\varepsilon U^2, & U &= \frac{-1 + \sqrt{4\varepsilon(X_1 + X_2) + 1}}{2\varepsilon}.\end{aligned}\tag{8}$$

The eigenfrequencies of the oscillatory circuits without regard to dissipation are assumed to satisfy, at least approximately, the parametric resonance condition (1).

Fig. 3 shows time dependences of U_1 and U_2 , obtained by numerical solution of equations (8).¹ Comparing the graphs in fig. 2 and fig. 3, we see some correspondence of the observed dynamics. In both cases, we have chaotic implementations that contain similar-looking fragments of signals. Herein, there is a match on typical scales of time and voltage. Calculating the Lyapunov exponents by joint numerical solution of equations (8) and corresponding equations in variations based on the known Gram–Schmidt orthogonalization algorithm [8, 9] gives² $\lambda_1 = 0.00956 \pm 0.00001$, $\lambda_2 = 0.0000 \pm 0.00001$, $\lambda_3 = -0.00854 \pm 0.00001$, $\lambda_4 = -1.9506 \pm 0.0001$.

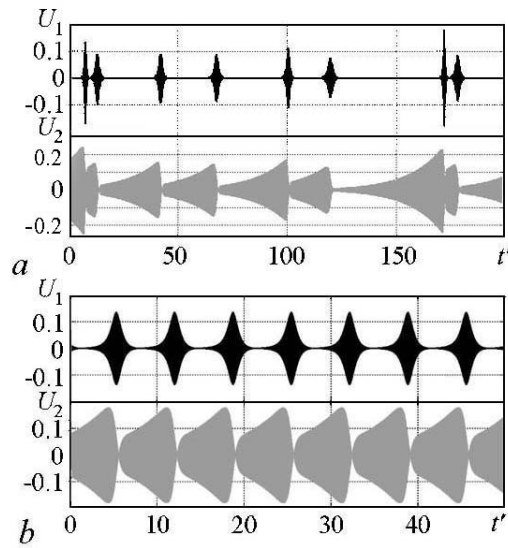


Fig. 3. Typical type of time dependences of voltage on capacitors C_1 and C_2 obtained by numerical solution of equations (8) at $\varepsilon = 0.1$: a – chaotic regime $\gamma = 0.026$; b – periodic regime $\gamma = 0.2$

¹For the scheme shown in Fig. 1 the change of parameter γ is provided by setting the resistance $R_g = 500$ k Ω . Other ratings of the scheme correspond to those shown in Fig. 1.

²Calculations of the Lyapunov exponents were carried out on intervals for normalized time of 3500 duration with calculation of average value and standard deviation for 50 realizations. The mean squared deviation is a measure of accuracy for predictions.

A positive values implies presence of chaos, characterized by an exponential increase in deviation from the reference trajectory of the attractor with a small perturbation of initial conditions. The second Lyapunov exponent, equal to zero within the accuracy of calculation error, is relatable to shift perturbation along the trajectory. The third and fourth exponents are negative and responsible for convergence of trajectories to the attractor. The fact that the parameters sum is negative indicates a compression of the phase volume in three-dimensional state space. It is consistent with the analytical calculation of the vector field divergence given by the right-hand sides of equations (8): $\text{div } \mathbf{F} = \partial_x f_x + \partial_y f_y + \partial_z f_z + \partial_w f_w = \gamma - 1 = -0.974$. Estimating the dimension of the attractor according to the Kaplan–Yorke formula gives the following value $D = 3 + \lambda_1/|\lambda_3| \approx 3.005$.

Fig. 4 shows dependence of four parameters of the Lyapunov exponents (8) on parameter γ . According to this figure, at $\gamma < 0.1$ the higher exponent is positive (albeit of small value), which indicates presence of chaotic dynamics. But for the values of parameter $\gamma > 0.1$ the first and second exponents are equal to zero, and the third and fourth ones are negative, that is, in this area a periodic regime is realized. The corresponding dependences of the values U_1 and U_2 , obtained in the numerical solution of equations (8) are shown in Fig. 3, *b* and the Lyapunov exponents are equal: $\lambda_1 = 0.0000 \pm 0.0001$, $\lambda_2 = 0.0000 \pm 0.0001$, $\lambda_3 = -0.3539 \pm 0.0001$, $\lambda_4 = -1.2486 \pm 0.0001$. Herein, as one can see from the graph of the higher Lyapunov exponent, there are ravines (regularity windows) also accompanied by emissions or ravines on the graphs of other exponents. This type of graph of the Lyapunov exponents depending on a parameter is typical for one-dimensional maps with a quadratic extremum and many other dissipative systems, including the Hénon map and the Rössler model, that demonstrate transition to chaos through a cascade of period doubling bifurcations [10, 11] and are associated with the concept of quasi-attractor [12, 13].

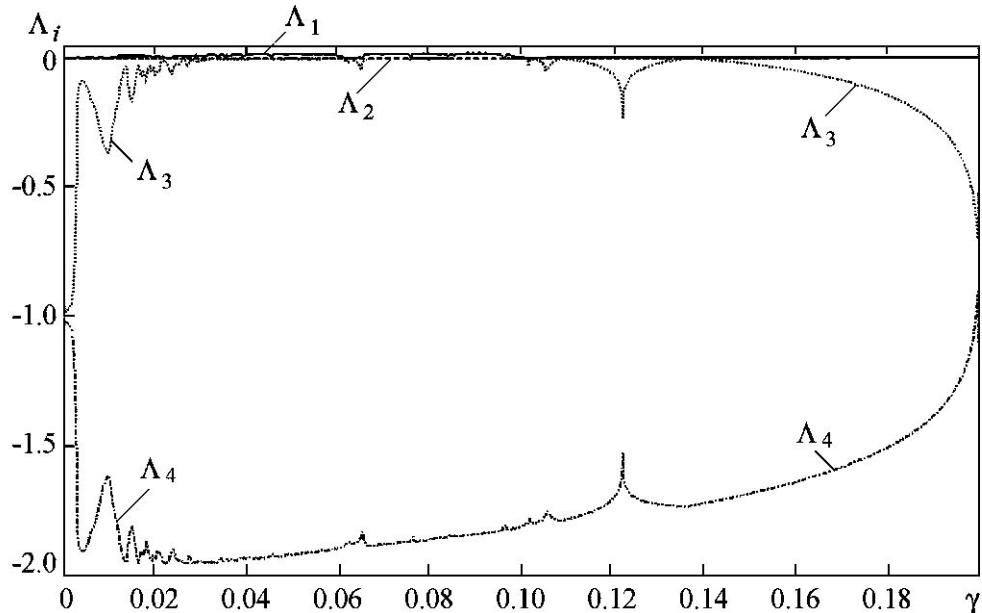


Fig. 4. Numerically graphs of four Lyapunov exponents for equations (8) at the value of the parameter $\varepsilon = 0.1$

3. Equations for slowly varying amplitudes

To obtain the equations in a form allowing a comparison with the Vyshkind–Rabinovich model, the method of slow complex amplitudes should be used.

To begin with, we rewrite the equations, taking into consideration only those terms that can be responsible for the resonance mode interactions at the assumed frequency ratio. According to (3) we have

$$\begin{aligned}\frac{d^2U_1}{dt^2} + 2\frac{dU_1}{dt} + \Omega_1^2U_1 &= -\frac{1}{2}\varepsilon\frac{d^2U^2}{dt^2}, \\ \frac{d^2U_2}{dt^2} - 2\gamma\frac{dU_2}{dt} + \Omega_2^2U_2 &= -\frac{1}{2}\varepsilon\frac{d^2U^2}{dt^2},\end{aligned}\quad (9)$$

here and further primes on the time variable are omitted for brevity.

In the first and second equations, taking into consideration only the resonance terms, we should assume, respectively,

$$\frac{1}{2}U^2 \approx U_1U_2, \quad \frac{1}{2}U^2 \approx \frac{1}{2}U_1^2, \quad (10)$$

and, moreover, it is possible to replace the operation of second derivation in the right parts by multipliers $(-\Omega_{1,2}^2)$. As a result, we have

$$\begin{aligned}\ddot{U}_1 + 2\dot{U}_1 + \Omega_1^2U_1 &= \varepsilon\Omega_1^2U_1U_2, \\ \ddot{U}_2 - 2\gamma\dot{U}_2 + \Omega_2^2U_2 &= \frac{1}{2}\varepsilon\Omega_2^2U_1^2.\end{aligned}\quad (11)$$

We seek solution in the form

$$\begin{aligned}U_1 &= A_1e^{i\omega_1t} + A_1^*e^{-i\omega_1t}, \quad \dot{U}_1 = i\omega_1A_1e^{i\omega_1t} - i\omega_1A_1^*e^{-i\omega_1t}, \\ U_2 &= A_2e^{i\omega_2t} + A_2^*e^{-i\omega_2t}, \quad \dot{U}_2 = i\omega_2A_2e^{i\omega_2t} - i\omega_2A_2^*e^{-i\omega_2t}\end{aligned}\quad (12)$$

that implies fulfillment of additional conditions for the introduced complex amplitude variables A_1 and A_2

$$\dot{A}_1e^{i\omega_1t} + \dot{A}_1^*e^{-i\omega_1t} = 0, \quad \dot{A}_2e^{i\omega_2t} + \dot{A}_2^*e^{-i\omega_2t} = 0. \quad (13)$$

Reference frequencies $\omega_{1,2}$ we define as

$$\omega_1 = \Omega_1, \quad \omega_2 = 2\Omega_1. \quad (14)$$

Here with, $\omega_2 \approx \Omega_2$, but the exact equality is not assumed as the relevant mismatch will be taken into consideration. Substituting in equations (11) gives

$$\begin{aligned}2i\omega_1\dot{A}_1 + 2i\omega_1A_1 &= \varepsilon\Omega_1^2A_1^*A_2, \\ 2i\omega_2\dot{A}_2 - 2i\omega_2\gamma A_2 - (\Omega_2^2 - \omega_2^2)A_2 &= \frac{1}{2}\varepsilon\Omega_2^2A_1^2,\end{aligned}\quad (15)$$

or

$$\begin{aligned}\dot{A}_1 + A_1 &= -\frac{1}{2}i\varepsilon\Omega_1A_1^*A_2, \\ \dot{A}_2 - \gamma A_2 - i\delta A_2 &= -\frac{1}{4}i\varepsilon\Omega_2A_1^2,\end{aligned}\quad (16)$$

where

$$\delta = \frac{\omega_2^2 - \Omega_2^2}{2\omega_2} = \frac{(2\Omega_1 - \Omega_2)(2\Omega_1 + \Omega_2)}{2\omega_2} \approx 2\Omega_1 - \Omega_2 \quad (17)$$

is a frequency mismatch.

Now we carry out renormalization

$$A_1 = \frac{2\sqrt{2}}{\varepsilon\sqrt{\Omega_1\Omega_2}}a_1 \approx \frac{2}{\varepsilon\Omega_1}a_1, \quad A_2 = \frac{2}{\varepsilon\Omega_1}a_2 \quad (18)$$

and get final formula

$$\begin{aligned} \dot{a}_1 + a_1 &= -ia_1^*a_2, \\ \dot{a}_2 - \gamma a_2 - i\delta a_2 &= -ia_1^2. \end{aligned} \quad (19)$$

This is just the system of shortened equations for the model (8). To obtain the Vyshkind–Rabinovich model, we make a substitution

$$a_1 = Ae^{i\varphi}, \quad a_2 = Be^{i\Phi}, \quad \Phi = \phi - 2\varphi \quad (20)$$

in equations (19). Here A and B are real variables, and Φ is a phase difference. Then we get

$$\begin{aligned} \dot{A} &= AB \sin \Phi - A, \\ \dot{B} &= -A^2 \sin \Phi + \gamma B, \\ \dot{\Phi} &= (2B - A^2 B^{-1}) \cos \Phi + \delta. \end{aligned} \quad (21)$$

If now enter new variables

$$X = -B \sin \Phi, \quad Y = -B \cos \Phi, \quad Z = A^2, \quad (22)$$

then equations (21) will take the form

$$\begin{aligned} \dot{X} &= Z + \delta Y - 2Y^2 + \gamma X, \\ \dot{Y} &= -\delta X + 2XY + \gamma Y, \\ \dot{Z} &= -2Z(X + 1), \end{aligned} \quad (23)$$

which corresponds to the Vyshkind–Rabinovich model obtained in [1] for describing turbulence in dissipative environment with hydrodynamic type of nonlinearity.

4. Dynamics of the short equation system

Now we consider the dynamics of the short equation system (19). Fig. 5 shows the numerical dependence of four Lyapunov exponents (19) on parameter γ . Note that dependence of the Lyapunov exponents in the initial system (8) and in the short equations (19) are very close, except for the region of small values of parameter $\gamma < 0.03$.

Fig. 6 shows time dependence of slow amplitudes $|a_1|$ and $|a_2|$ in chaotic and periodic regimes. Its implementations demonstrate typical behavior for these modes. The Lyapunov exponents for the chaotic regime are: $\lambda_1 = 0.009593 \pm 0.000001$, $\lambda_2 = 0.000000 \pm \pm 0.000001$, $\lambda_3 = 0.000000 \pm 0.000001$, $\lambda_4 = -1.957592 \pm 0.000001$; for periodic regime: $\lambda_1 = 0.000000 \pm 0.000001$, $\lambda_2 = 0.000000 \pm 0.000001$, $\lambda_3 = -0.145560 \pm 0.000001$, $\lambda_4 = -1.454439 \pm 0.000001$.

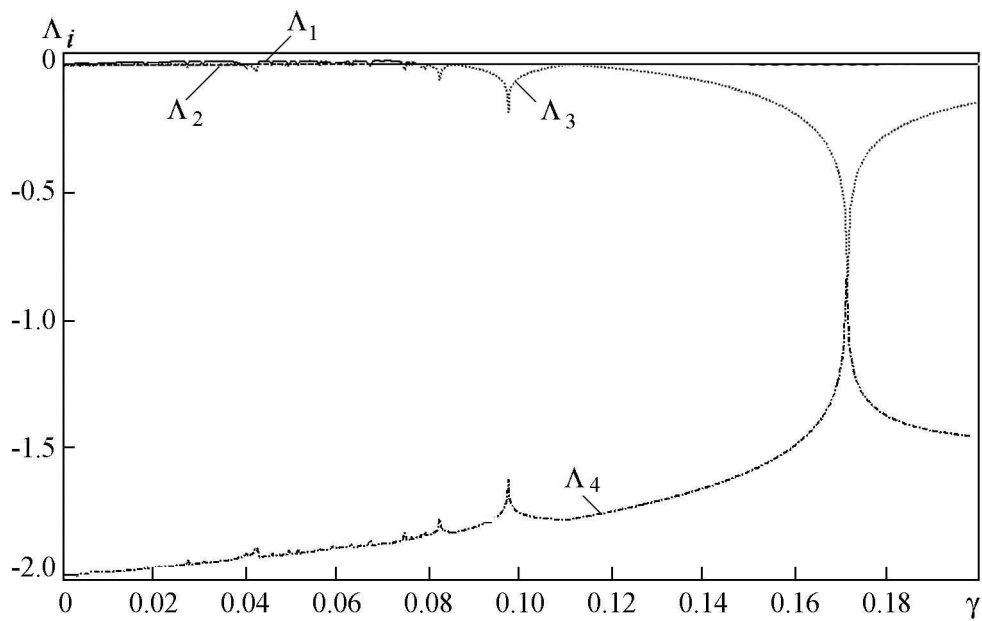


Fig. 5. Numerically graphs of four Lyapunov exponents of equations (19) at the value of the parameter $\delta = 0.184$

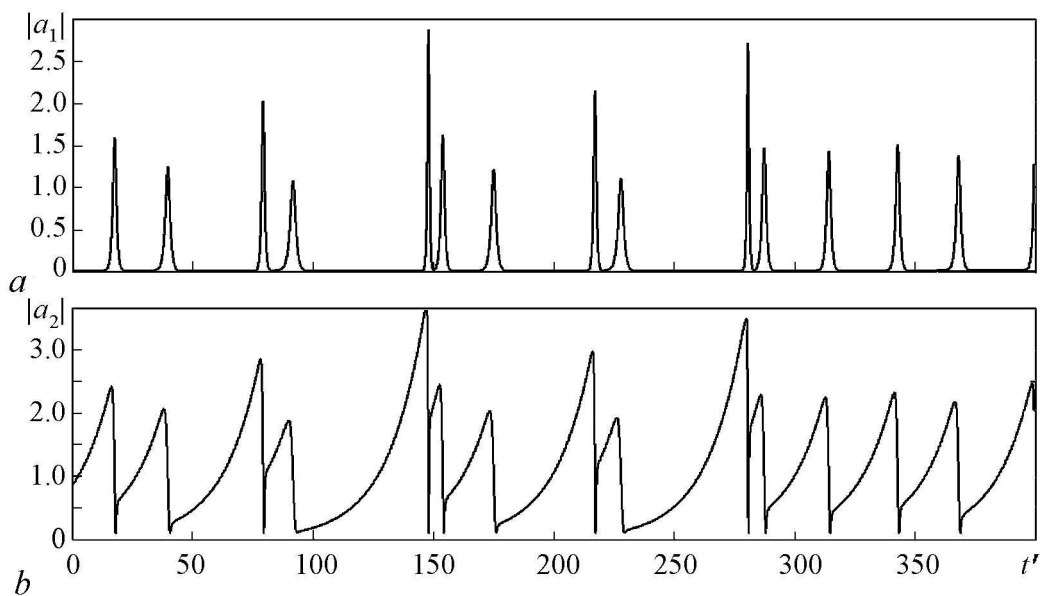


Fig. 6. Typical type of time dependences of $|a_1|$ and $|a_2|$ system of truncated equations (19). a – chaotic regime $\gamma = 0.026$; b – periodic regime $\gamma = 0.2$. $\varepsilon = 0.1$

5. Regular and chaotic dynamics of the Vyshkind–Rabinovich model

Let us consider the Vyshkind–Rabinovich model system (23) and construct a chart of dynamical regimes on the parameter plane (δ, γ) . The procedure consists in scanning and enumeration of grid nodes with certain step for two parameters. At each point, about 500 iterations of Poincaré map defined for the system (23) are performed using a secant surface in phase space $S = Z + \delta Y - 2Y^2 + \gamma X = 0$ (going in the direction of rise S). Based on the results of the last iteration steps, the presence or absence of the repetition period of the states in the Poincaré section from 1 to 16 with some initially specified level of error is analyzed. When periodicity is detected, the corresponding pixel in the chart is marked in a color defined by the state repetition period; otherwise the pixel is marked in black. Then we proceed to the analysis of the next point on the parameter plane. Herewith, at a new point it is reasonable to set the initial conditions obtained at the previous point as a result of iterations («scanning with inheritance»), which accelerates convergence to the steady-state dynamics. The correspondent map is shown in Fig. 7. On the periphery of the figure there are portraits of attractors corresponding to the points marked on the parameter plane.

Note that the map of dynamic regimes is typical for dynamic systems with transition to chaos through a cascade of period doubling bifurcations. The attractor in the chaos region is similar to the Rössler attractor [8, 10]. Calculation for the chaotic regime gives the following results: $\lambda_1 = 0.00961 \pm 0.00001$, $\lambda_2 = 0.00000 \pm 0.00001$, $\lambda_3 = -1.95760 \pm 0.00001$; for the period mode 1 the results are the following: $\lambda_1 = 0.000000 \pm 0.000001$, $\lambda_2 = -0.14556 \pm 0.00001$, $\lambda_3 = -1.45444 \pm 0.00001$. The dimension of the chaotic attractor is $D = 2 + \lambda_1/|\lambda_3| \approx 2.004909$.

Fig. 8 shows the dependence of three Lyapunov exponents of the model (23) on parameter γ . Note that at the qualitative level dependence of the Lyapunov exponents

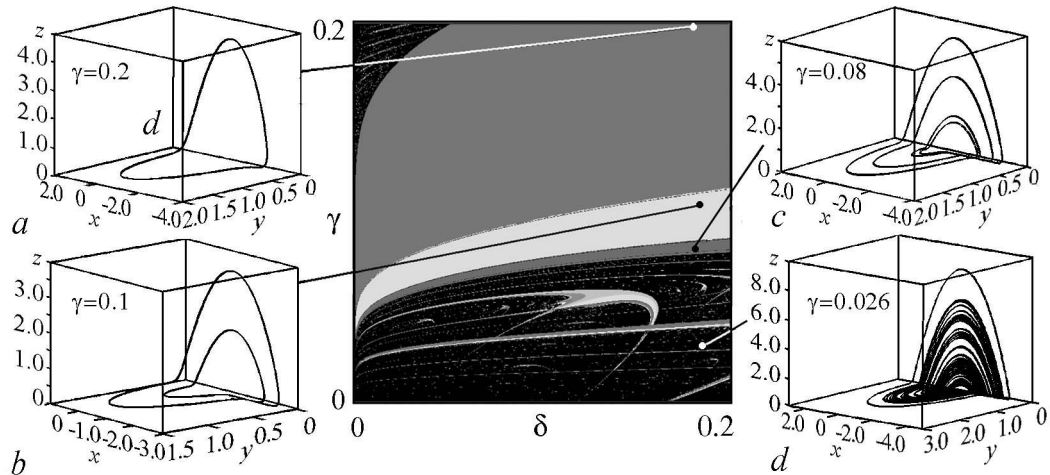


Fig. 7. Chart of dynamical regimes of model (23) at the parameter plane (δ, γ) and attractors plotted at the marked points; for all attractors $\delta = 0.184$

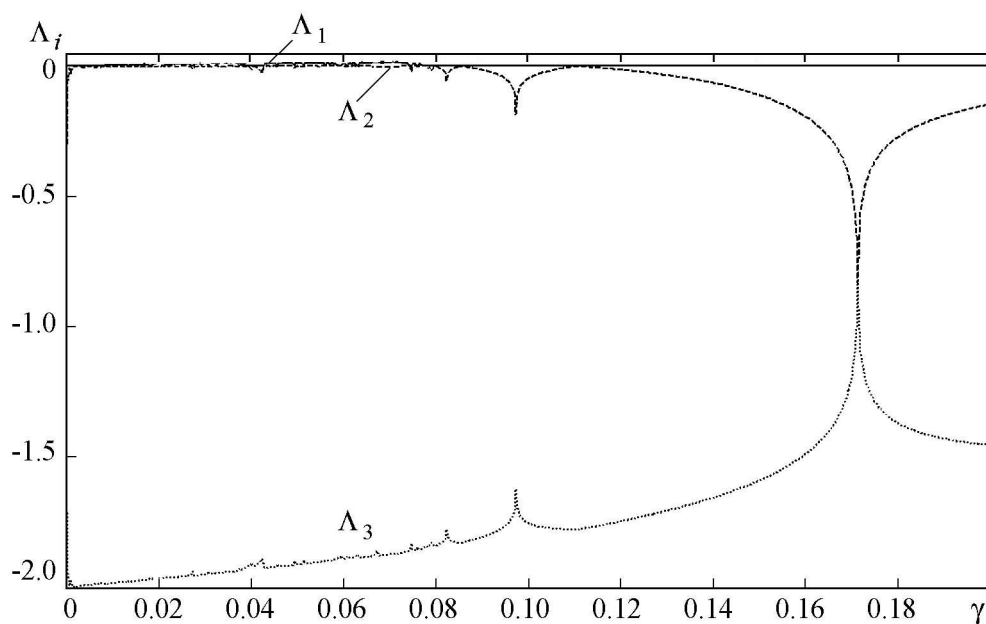


Fig. 8. Graphs of three Lyapunov exponents of equations (23) at the value of the parameter $\delta = 0.184$

in the initial system (8) and the Vyshkind–Rabinovich model (23) are identical (compare Fig. 4 and Fig. 8). In both cases, there is chaos in the region of small values of parameter γ , which is due to the limit cycle emerging from the cascade of period doubling bifurcations.

Conclusion

This paper analyzes the scheme of parametric chaos generator basis on two LC-circuits, one of which includes negative conductivity. We have obtained the equations describing the dynamics of the system, including the equations directly describing the oscillations of voltages and currents in oscillatory circuits, the amplitude equations and the equations in the form of the Vyshkind–Rabinovich model. The dynamics of these models has been numerically studied using methods of the dynamic chaos theory: time dependences of dynamic variables, portraits of attractors, the Lyapunov exponents depending on parameters. Also, for the Vyshkind–Rabinovich model we have created a map of dynamical regimes on the parameter plane. The results obtained for all models correlate well. We have shown that all systems demonstrate transition to chaos through a sequence of period doubling bifurcations with a decrease of one of the parameters. The resulting chaotic attractor has a structure similar to the Rössler attractor.

We have carried out a schematic simulation of the system using the software product Multisim; the results of this simulation are consistent with the results of numerical analysis of the system.

Our analysis shows that it is possible to use the considered electronic circuit for analog simulation of oscillatory and wave phenomena in systems to which the model representations developed by S.Y. Vyshkind and M. I. Rabinovich are applicable.

Development of the scheme of electronic generator, the output equations and circuit simulation (sections 1, 2 and 3) are performed with the support of Russian Foundation for Basic Research grant No. 15-02-02893. Numerical calculations, processing and interpretation of the results (sections 4, 5) were carried out at the expense of the Russian Science Foundation grant (project No. 17-12-01008).

References

1. Vyshkind S.Y., Rabinovich M.I. The phase stochastization mechanism and the structure of wave turbulence in dissipative media. *Soviet Journal of Experimental and Theoretical Physics*, 1976, vol. 44, pp. 292–299.
2. Demidov V.E., Kovschikov N.G. Mechanism of occurrence and stochastization of self-modulation of intense spin waves. *Technical Physics*, 1999, vol. 69, iss. 8, pp. 100–103.
3. Romanenko D.V. Chaotic microwave pulse train generation in self-oscillatory system based on a ferromagnetic film. *Izvestiya VUZ, Applied Nonlinear Dynamics*, 2012, Vol. 20, iss. 1, pp. 67–74 (in Russian).
4. Wersinger J.M., Finn J.M., Ott E. Bifurcation and «strange» behavior in instability saturation by nonlinear three-wave mode coupling. *The Physics of Fluids*, 1980, vol. 23, no. 6, pp. 1142–1154.
5. Savage C.M., Walls D.F. Optical chaos in second-harmonic generation. *Journal of Modern Optics*, 1983, vol. 30, no. 5, pp. 557–561.
6. Lythe G.D., Proctor M.R.E. Noise and slow-fast dynamics in a three-wave resonance problem. *Physical Review E*, 1993, vol. 47, no. 5, 3122.
7. Kuznetsov S.P. Lorenz type attractors in electronic parametric generator and its transformation outside the accurate parametric resonance. *Izvestiya VUZ, Applied Nonlinear Dynamics*, 2016, vol. 24, iss.3, pp. 68–87 (in Russian).
8. Kuznetsov S.P. *Dynamical Chaos*. Moscow: Fizmatlit, 2006. 356h. (in Russian).
9. Benettin G., Galgani L., Giorgilli A., Strelcyn J.-M. Lyapunov characteristic exponents for smooth dynamical systems and for Hamiltonian systems: A method for computing all of them. *Meccanica*, 1980, Vol. 15, pp. 9–20.
10. Rössler O.E. Continuous chaos: four prototype equations. *Ann. New York Academy of Sciences*, 1979, vol. 316, pp. 376–392.
11. Hénon M. A two-dimensional mapping with a strange attractor. *Commun. Math. Phys*, 1976, vol. 50, pp. 69–77.
12. Afraimovich V.S. Strange attractors and quasiattractors. *Nonlinear and turbulent processes in physics*, 1984, vol. 1, pp. 1133–1138.
13. Shilnikov L.P. Bifurcations and strange attractors. *Vestnik Nizhegorodskogo Universiteta*, 2011, no. 4(2), pp. 364–366 (in Russian).